Open Access

Asian Journal of Environmental Research
E-ISSN: 3047-4930
DOI: https://doi.org/10.69930/ajer.v2i1.274
Research Article

Vol. 2 (1), 2025
Page: 29-47

Analysis the Effect of Control Valve Opening on Loading Crude Glycerine Water Pump Motor at PT. Unilever Oleochemical Indonesia

Dwiki Darma Nuriono Brid, Zuraidah Tharo *, Pristisal Wibowo

Department of Electrical Engineering, Faculty of Science and Technology, Pancabudi University, Indonesia
*Email (corresponding author): zuraidahtharo@dosen.pancabudi.ac.id

Abstract. *In the palm oil industry, three-phase induction motors have a very important role in the production process. One of the problems that arises is the quality of the loading power on the motor which can make the motor performance less than optimal. In this study, an analysis and calculation of the power of a three-phase induction motor were carried out with the condition of opening the control valve in stages from 0% to 100%. The motor to be discussed is a three-phase induction motor that works as a pump driver for transferring crude glycerine water to the tank farm at the fatty acid 2 plant at PT. Unilever Oleochemical Indonesia. By using the observation method in researching to obtain measurement data, the variables taken are changes in current, power factor, and input power. From the results of this study, the output power value and power efficiency on the motor were obtained when the valve was opened at 0%-100%, at the highest valve opening of 100%, the motor output power was 4.39 KW with a power efficiency on the motor of 95%, at the lowest valve opening, the motor output power was 3.22 KW with an efficiency value obtained 95%.*

Keywords: *Three-phase induction motor, current, efficiency, valve, opening*

1. Introduction

In this modern industrial era, especially in the palm oil industry in Indonesia, there have been many advances and technological developments, one of which is electric motors as a source of driving power that is very much needed, starting from engine drives, pumps, conveyors, etc. So many innovations have emerged to control electric motors to meet the increasing demand and needs. PT. Unilever Oleochemical Indonesia is a company engaged in the processing of palm oil, especially oleochemicals with raw materials CPKO (Crude Palm Kernel Oil) or CPO (Crude Palm Oil), and produces products such as Glycerine and Fatty Acid.

In the palm oil production process, the existence of electric motors is very much needed, starting from pump drives for liquid fluid transfer, to product mixers, conveyors, and several other needs.

One of the innovations in controlling the transfer pump motor uses the help of a "Control Valve" to electronically control the opening of the valve and control the loading on the transfer pump motor so that there is no overload in filling the tank and facilitating gradual filling to reach the desired set point, this innovation is also considered to have quite

Received: 18 December 2024 / Accepted: 30 January 2025 / Available online: 31 January 2025

good work efficiency so that it can reduce the factory's need for the number of human workers which has an impact on saving factory production expenses.

2. Methods

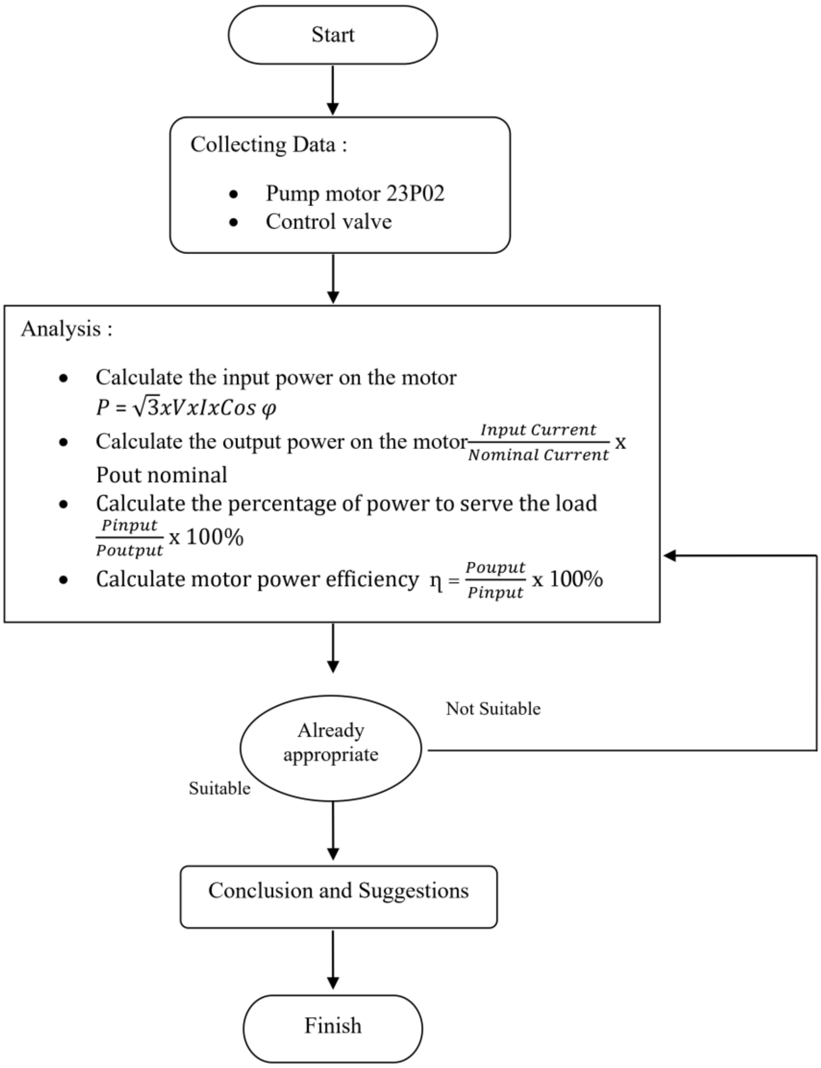

Figure 1. Research flow

The object of this research is the crude glycerine water pump motor and control valve. The researcher will do several things in this research, here are the details of the things that the research will do.

1. Collecting data related to the pump motor specifications.
2. Collecting data related to the specifications of the control valve used.
3. Carrying out the opening command for each percentage of the control valve via the DCS monitor.
4. Taking measurements with an ampere clamp in the control room of the crude glycerine water pump motor 23P02 for each percentage of the control valve opening with a valve opening range of 0% - 100%.
5. Recording data related to the motor load that is read on the ampere clamp for each control valve opening.

6. Conducting analysis, calculations and discussions related to the data that has been taken and drawing conclusions from the research that has been carried out.

2.1. Three Phase Induction Motor

Three-phase induction motor is an electrical device that converts electrical energy into mechanical energy, where the electricity converted is three-phase electricity. Induction motors are often also called asynchronous motors. Induction motors generally convert electrical energy into mechanical energy in the rotating part of the motor.

In induction motors, the rotor does not obtain electrical energy through conduction, but obtains electrical energy through induction, as in the secondary winding of a transformer, the rotor obtains electrical energy from its primary winding. Therefore, induction motors can also be called resolvers.

Induction motors are the most widely used AC motors in industry. This is because the motor structure is strong, simple and does not require much maintenance. In addition, the motor also provides good efficiency and constant rotation for every load change.

2.2. Working Principle of Three Phase Induction Motor

The operation of a three-phase induction motor can be described as follows:

1. If a three-phase source is connected to the stator coil of a three-phase induction motor, a rotating field will arise between the stator and rotor circles at synchronous speed.
2. This rotating field will cut the rotor conductor rod.
3. As a result, an EMF will be generated in the rotor coil.
4. Because the rotor coil is a closed circuit, the EMF (E2) will produce a rotor current (I2).
5. The flow of rotor current (I2) in the magnetic field produces a force (F) on the rotor.
6. If the initial torque generated by the force (F) on the rotor is strong enough to carry the load, the rotor will rotate following the direction of the movement of the stator rotating field.
7. In order for the rotor EMF to remain generated in the rotor, a difference in relative rotation between the stator rotating field (NS) and the rotor rotation (Nr) is required.
8. The difference in rotational speed (NS) and (Nr) is called Slip.
9. If the rotational speed (NS) is the same as the rotor rotation (Nr), then the rotor EMF is not induced and no current flows in the rotor coil, thus no torque is generated.
10. Torque will arise if the rotor puran is less than the stator field rotation. From the way this motor works, the Induction Motor is also called an Asynchronous or A-Synchronous Motor.

2.3. Calculating Motor Input Power

From the results of measuring the voltage and current flowing at the motor input, the author can then find the power requirements absorbed by the motor at each valve opening as follows:

$$P = \sqrt{3}\ xVxIxCos\varphi$$

The flowing voltage is 380V with a power factor ($Cos\varphi$) of 0.84

CC BY SA

Power factor or cos phi is only found in alternating current (AC). When electric current is passed from a generator to a network, electrical energy transfer will occur. the power factor value will always be below 1. This shows that the amount of active power is always smaller than the apparent power. This value also shows how effective the use of electricity is. the closer to the number 1, it can be said to be efficient, and vice versa.

One of the things that affects the power factor value is reactive power. The definition of reactive power is the power released to turn on the inductive load. It can also be interpreted as power lost because it is not used for resistive loads.

2.4. Calculating Motor Output Power

Because there is a change in current at each valve opening, the motor output power will also change, therefore before calculating the motor efficiency from each valve opening, it must be known how much output power is on the motor at each valve opening, for that it is necessary to know the percentage between the current on the name plate and the incoming current, so it needs to be traced in the following way:

$$\frac{InputCurrent}{NominalCurrent} \text{ x Pout nominal}$$

2.4. Motor Power Percentage

Percentage of power to serve the load From the measurement and calculation results above, it can be seen the percentage of power usage on the motor to serve the valve opening load starting from 0% to 100% opening. Calculate the percentage of power usage used to serve each valve opening percentage.

$$\frac{Pinput}{Poutput} \text{ x } 100\%$$

2.5. Calculating Power Efficiency

By calculating the power efficiency of the motor, the output power is obtained at each valve opening. Then, to find out the motor power efficiency obtained at each valve opening percentage, it is as follows using the formula

$$\eta = \frac{Poutput}{Pinput} \text{ x } 100\%$$

Information

η = Efficiency (%)

Pout = Induction motor output power (Watt)

Pin = Induction motor output power (Watt)

2.6. Motor Specification Data 23P02 Crude Glycerine Water

The crude glycerine water pump also uses a TOR (Thermal Overload Relay) which is set at 10.4A according to the instructions on the motor nameplate.

Figure 2. Name plate motor 23P02

Figure 3. Pump motor 23P02

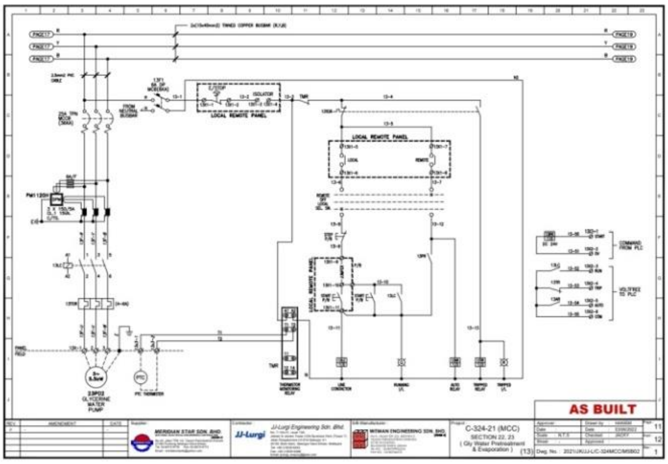

Figure 4. Wiring diagram 23P02

BY SA

Table 1. Motor specification

Unit Specification	**Information**
Manufacturer Name	SIEMENS
Type	Induction Motor
Serial Number	2203/2422971-008-001
Weight	50 Kg
Phase	3~
Frequency	50 Hz
Working Voltage	400/690
Power	5,5 KW
Current	10,4/6,0A
IP	55
Power Factor/cos phi	0,84
Efficiency	90,9%
Rotation/min	2960 rpm
INS.Class	155(F)

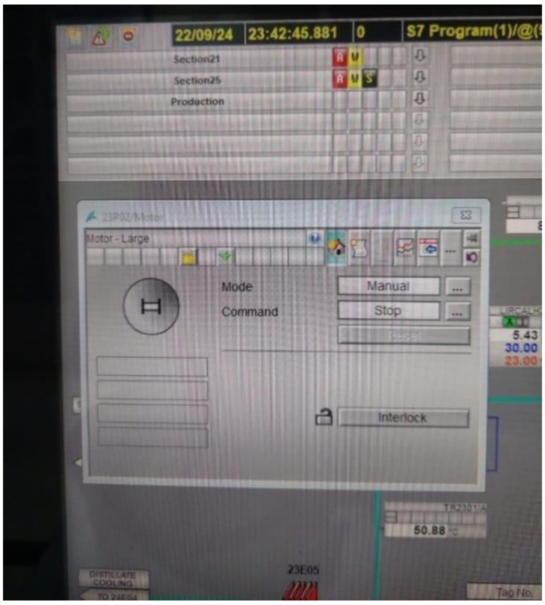

Figure 5. 23P02 display on DCS monitor

2.7. LV2301 Control Valve Specification Data

In the industrial sector, control valves play a very important role, especially in the control process in modern factories today. Control valves are generally used to control the flow rate of fluids and gases. This tool is very important for the continuity of a better factory production process. Such control is usually used for several processes, for example: Energy exchange, pressure reduction, pressure control, pressure filling and the simplest for filling tanks.

The working principle of the control valve is that the control valve is controlled by providing energy input in the form of compressed air / Instrument Air, electric power, hydraulics, input to control the control valve is issued by the controller which is usually called the manipulated variable.

CC BY SA

For compressed air / Instrument Air the standard signal is 3-15 Psi, for electric it is 4-20 mA current. These signals are used to move the stem from fully open to fully closed called bench set. The control valve has very good accuracy to be controlled.

Table 2. LV2301 control valve specification

Unit Specification	Information
Manufacturer Name	SAMSON
Model Number	3725-1100000000
Power Supply	4 to 20 mA DC
Class	CL 150
Temperature	-25 °C to 80°C
Degree of protecion	IP 66
Supply max	7 bar/105 psi
Serial Number	500943233
Connection size	M20 x 1.5

Figure 6. LV2301 in the field

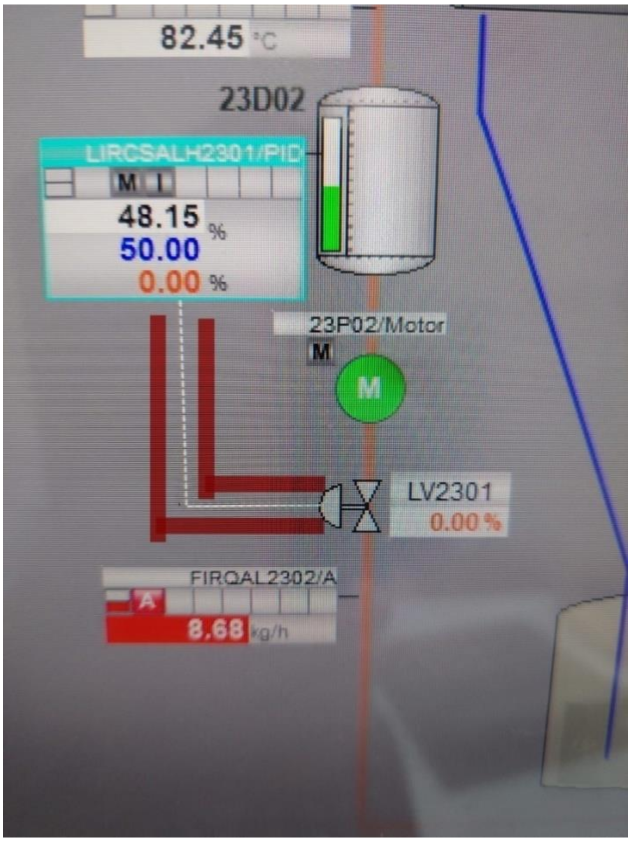

Figure 7. LV2301 Interlock with level control

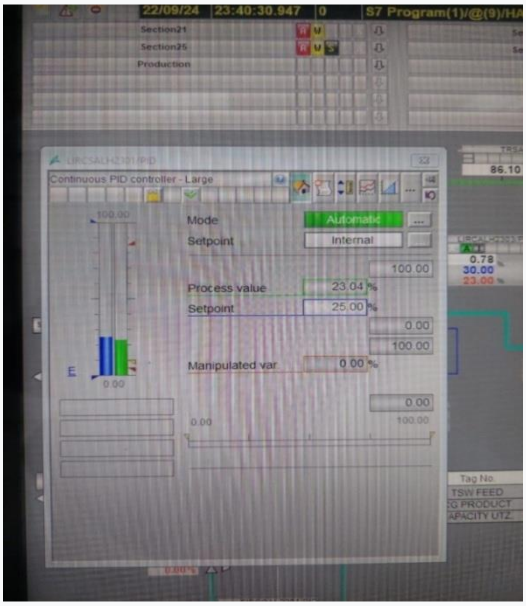

Figure 8. Set point and opening control valve in balance condition

3. Results and Discussion

The voltage can remain stable even though the current changes because of the presence of a voltage source designed to maintain its output voltage, as well as the presence of voltage regulator components in many devices. This concept is very important in understanding how electrical systems work.

CC BY SA

Table 3. Voltage and current measurement results

No.	Valve Opening	Voltage (V)			Current (A)		
		R	S	T	R	S	T
1.	0%	380	380	380	6,1	6,1	6,1
2.	10%	380	380	380	6,2	6,2	6,2
3.	20%	380	380	380	6,3	6,3	6,3
4.	30%	380	380	380	6,4	6,4	6,4
5.	40%	380	380	380	6,6	6,6	6,6
6.	50%	380	380	380	6,7	6,7	6,7
7.	60%	380	380	380	6,9	6,9	6,9
8.	70%	380	380	380	7,3	7,3	7,3
9.	80%	380	380	380	7,7	7,7	7,7
10.	90%	380	380	380	8,0	8,0	8,0
11.	100%	380	380	380	8,3	8,3	8,3

3.1. Calculating Motor Input Power

From the results of measuring the voltage and current flowing at the motor input, the author can then find the power requirements absorbed by the motor at each valve opening as follows. $P = \sqrt{3}\ xVxIxCos\varphi$The flowing voltage is 380V with a power factor ($Cos\varphi$) of 0.84

0% opening with 6.1A current

$P = \sqrt{3}\ xVxIxCos\varphi$

=1,73 x 380 x 6,1 x 0,84

=3.368,51 W

10% opening with 6.2A current

$P = \sqrt{3}\ xVxIxCos\varphi$

=1,73 x 380 x 6,2 x 0,84

=3.432,73 W

20% opening with 6.3A current

$P = \sqrt{3}\ xVxIxCos\varphi$

=1,73 x 380 x 6,3 x 0,84

=3.478,96 W

30% opening with 6.4A current

$P = \sqrt{3}\ xVxIxCos\varphi$

=1,73 x 380 x 6,4 x 0,84

=3.534,18 W

40% opening with 6.6A current

$P = \sqrt{3}\ xVxIxCos\varphi$

=1,73 x 380 x 6,6 x 0,84

=3.644,62 W

50% opening with 6.7A current

$P = \sqrt{3}\ xVxIxCos\varphi$

=1,73 x 380 x 6,7 x 0,84

=3.699,84 W

60% opening with 6.9A current

CC BY SA

$P = \sqrt{3}\ xVxIxCos\varphi$
=1,73 x 380 x 6,9 x 0,84
=3.810,29 W
70% opening with 7.3A current
$P = \sqrt{3}\ xVxIxCos\varphi$
=1,73 x 380 x 7,3 x 0,84
=4.031,17 W
80% opening with 7.7A current
$P = \sqrt{3}\ xVxIxCos\varphi$
=1,73 x 380 x 7,7 x 0,84
=4.252,06 W
90% opening with 8.0A current
$P = \sqrt{3}\ xVxIxCos\varphi$
=1,73 x 380 x 8,0 x 0,84
=4.417,72 W
100% opening with 8.3A current
$P = \sqrt{3}\ xVxIxCos\varphi$
=1,73 x 380 x 8,3 x 0,84
=4.583,39 W

The following shows the calculation results in table form.

Table 4. Input power and calcucaltion results

No.	Control Valve (%)	Voltage (V)	Current (A)	Power (W)
1	0	380	6,1	3.368,51
2	10	380	6,2	3.432,73
3	20	380	6,3	3.478,96
4	30	380	6,4	3.534,18
5	40	380	6,6	3.644,62
6	50	380	6,7	3.699,84
7	60	380	6,9	3.810,29
8	70	380	7,3	4.031,17
9	80	380	7,7	4.252,06
10	90	380	8,0	4.417,72
11	100	380	8,3	4.583,39

3.2 Calculating Motor Output Power

To find out the output power of the motor, the following equation can be used.$\frac{InputCurrent}{Nominal\ Current}$ x Pout nominal . So it's obtained,
At 0% opening the current flowing is 6.1A so that we get
$\frac{6{,}1\ A}{10{,}4}$ x 5,5 KW
=3,22 KW
At 10% opening the current flowing is 6.2A so that we get

CC BY SA

$\frac{6,2A}{10,4}$ x 5,5 KW

=3,27 KW

At 20% opening the current flowing is 6.3A so that we get

$\frac{6,3A}{10,4}$ x 5,5 KW

=3,33 KW

At 30% opening the current flowing is 6.4A so that we get

$\frac{6,4\ A}{10,4}$ x 5,5 KW

=3,38 KW

At 40% opening the current flowing is 6.6A so that we get

$\frac{6,6A}{10,4}$ x 5,5 KW

=3,49 KW

At 50% opening the current flowing is 6.7A so that we get

$\frac{6,7A}{10,4}$ x 5,5 KW

=3,54 KW

At 60% opening the current flowing is 6.9A so that we get

$\frac{6,9A}{10,4}$ x 5,5 KW

=3,64 KW

At 70% opening the current flowing is 6.3A so that we get

$\frac{7,3A}{10,4}$ x 5,5 KW

=3,86 KW

At 80% opening the current flowing is 7.7A so that we get

$\frac{7,7\ A}{10,4}$ x 5,5 KW

=4,07 KW

At 90% opening the current flowing is 8.0A so that we get

$\frac{8,0\ A}{10,4}$ x 5,5 KW

=4,23 KW

At 100% opening the current flowing is 8.3A so that we get

$\frac{8,3\ A}{10,4}$ x 5,5 KW

=4,39 KW

Table 5. Output power calculation result

No.	Control Valve (%)	Voltage (V)	Input Power (W)	Output Power (KW)
1	0	380	3.368,51	3,22
2	10	380	3.432,73	3,27
3	20	380	3.478,96	3,33
4	30	380	3.534,18	3,38
5	40	380	3.644,62	3,49
6	50	380	3.699,84	3,54
7	60	380	3.810,29	3,64
8	70	380	4.031,17	3,86
9	80	380	4.252,06	4,07
10	90	380	4.417,72	4,23
11	100	380	4.583,39	4,39

3.3 Percentage of Power to Serve the Load

To find out the percentage of power, the following equation can be used.

$\frac{Pinput}{Poutput}$ x 100%

So it's obtained,

At 0% opening with input power of 3,368.51 W

$\frac{3.368{,}51\ \mathrm{W}}{5500\ W}$ x 100%

=61,2 %

At 10% opening with input power of 3.432,73 W

$\frac{3.432{,}73\ \mathrm{W}}{5500\ W}$ x 100%

=62,4 %

At 20% opening with input power of 3.478,96 W

$\frac{3.478{,}96\ \mathrm{W}}{5500\ W}$ x 100%

=63,2 %

At 30% opening with input power of 3.534,18 W

$\frac{3.534{,}18\ \mathrm{W}}{5500\ W}$ x 100%

=64,2 %

At 40% opening with input power of 3.644,62 W

$\frac{3.644{,}62\ \mathrm{W}}{5500\ W}$ x 100%

=66,2 %

At 50% opening with input power of 3.699,84 W

$\frac{3.699{,}84\ \mathrm{W}}{5500\ W}$ x 100%

=67,2 %

At 60% opening with input power of 3.810,29 W

$\frac{3.810{,}29\ \mathrm{W}}{5500\ W}$ x 100%

=69,2 %

At 70% opening with input power of 4.031,17 W

$\frac{4.031{,}17\ \mathrm{W}}{5500\ W}$ x 100%

CC BY SA

=73,2 %

At 80% opening with input power of 4.252,06 W

$\frac{4.252,06 \text{ W}}{5500\ W}$ x 100%

=77,3 %

At 90% opening with input power of 4.417,72 W

$\frac{4.417,72 \text{ W}}{5500\ W}$ x 100%

=80,3 %

At 100% opening with input power of 4.583,39 W

$\frac{4.583,39 \text{ W}}{5500\ W}$ x 100%

=83,3 %

From the results of the calculation of the percentage of power to serve the valve opening, it is known that at 0% valve opening, a power of 61.2% of the nominal motor power is required and the percentage continues to increase along with the maximum valve opening percentage, which is 100% with the percentage of power required being 83.3% of the nominal motor power.

3.4. Calculating Power Efficiency on a Motor

Thus, the output power has been obtained at each valve opening. Then, to find out the efficiency of the motor power obtained at each valve opening percentage, it is as follows, using the formula $\eta = \frac{Poutput}{Pinput}$ x 100% . So that we can then know the motor efficiency value at each valve opening.

At the time of opening 0%

Pout = 3,22 KW=3.220 W

Pin = 3.368,51

η=…?

$\eta = \frac{3.220}{3.368,51}$ x 100%

= 95%

At the time of opening 10%

Pout = 3,27 KW=3.270 W

Pin = 3.432,73

η=…?

$\eta = \frac{3.270}{3.432,73}$ x 100%

= 95%

At the time of opening 20%

Pout = 3,33 KW=3.330 W

Pin = 3.478,96

η=…?

$\eta = \frac{3.330}{3.478,96}$ x 100%

= 94%

At the time of opening 30%

Pout = 3,38 KW=3.380 W

CC BY SA

Pin = 3.534,18

η=…?

$$\eta = \frac{3.380}{3.534,18} \times 100\%$$

= 95%

At the time of opening 40%

Pout = 3,49 KW=3.490 W

Pin = 3.644,62

η=…?

$$\eta = \frac{3.490}{3.644,62} \times 100\%$$

= 95%

At the time of opening 50%

Pout = 3,54 KW=3.540 W

Pin = 3.699,84

η=…?

$$\eta = \frac{3.540}{3.699,84} \times 100\%$$

= 95%

At the time of opening 60%

Pout = 3,64 KW=3.640 W

Pin = 3.810,29

η=…?

$$\eta = \frac{3.640}{3.810,29} \times 100\%$$

= 95%

At the time of opening 70%

Pout = 3,86 KW=3.860 W

Pin = 4.031,17

η=…?

$$\eta = \frac{3.860}{4.031,17} \times 100\%$$

= 95%

At the time of opening 80%

Pout = 4,07 KW=4.070 W

Pin = 4.252,06

η=…?

$$\eta = \frac{4.070}{4.252,06} \times 100\%$$

= 95%

At the time of opening 90%

Pout = 4,23 KW=4.320 W

Pin = 4.417,72

η=…?

$$\eta = \frac{4.230}{4.417,72} \times 100\%$$

= 95%

At the time of opening 100%

Pout = 4,39 KW=4.390 W

CC BY SA

Pin = 4.583,39

η=…?

$\eta = \frac{4.390}{4.583,39} \times 100\%$

$= 95\%$

From the calculation results above, the following table shows the results of the calculation of the motor efficiency value for each open valve with percentage parameters.

Table 6. Motor efficiency calculation result

No.	Control Valve (%)	Input Power (W)	Output Power (KW)	Efficiency (%)
1	0	3.368,51	3,22	95
2	10	3.432,73	3,27	94
3	20	3.478,96	3,33	95
4	30	3.534,18	3,38	95
5	40	3.644,62	3,49	95
6	50	3.699,84	3,54	95
7	60	3.810,29	3,64	95
8	70	4.031,17	3,86	95
9	80	4.252,06	4,07	95
10	90	4.417,72	4,23	95
11	100	4.583,39	4,39	95

3.4 Overall Results

Based on the results of observations and calculations on the crude glycerine water pump motor at PT. Unilever Oleochemical Indonesia, it is known that at each valve opening, study results are obtained where changes in the current caused by changes in the valve opening will affect the loading on the motor, both input power, output power and power efficiency using the formula

$$\frac{InputCurrent}{NominalCurrent} \times \text{Pout nominal}$$

So that the change in output power can be known compared to the nominal power on the motor nameplate. After the output power is known, then the motor efficiency can be calculated at each valve opening using the formula

$$\eta = \frac{Poutput}{Pinput} \times 100\%$$

The following are the results of a study related to changes in valve openings that affect the load on the motor.

CC BY SA

Table 7. Overall results

No.	Control Valve (%)	Voltage (V)	Current (A)	Input Power (W)	Output Power (KW)	Efficiency (%)
1	0	380	6,1	3.368,51	3,22	95
2	10	380	6,2	3.432,73	3,27	95
3	20	380	6,3	3.478,96	3,33	94
4	30	380	6,4	3.534,18	3,38	95
5	40	380	6,6	3.644,62	3,49	95
6	50	380	6,7	3.699,84	3,54	95
7	60	380	6,9	3.810,29	3,64	95
8	70	380	7,3	4.031,17	3,86	95
9	80	380	7,7	4.252,06	4,07	95
10	90	380	8,0	4.417,72	4,23	95
11	100	380	8,3	4.583,39	4,39	95

From the case discussed, it is known that the factor that affects the efficiency of the crude glycerine water pump motor is the change in load due to the valve opening which affects the change in current at each percentage of valve opening.

Conclusions

Based on the analyzed data, it can be concluded that the current flowing through the crude glycerine water pump motor varies with the valve opening percentage, where at 0% opening the current is 6.1A and at 100% it increases to 8.3A. This variation in current is influenced by changes in load corresponding to different valve openings. Furthermore, these changes in current affect motor loading, including input power, output power, and power efficiency. Overall, a larger valve opening results in higher current flow, increased input power, and greater output power in the pump motor.

Funding

This research received no external funding.

Acknowledgments

Thank you to God Almighty, PT Unilever Oleochemical Indonesia, Mrs. Hj.Zuraidah Tharo, S.T, M.T. and my friends who supported me in completing this.

Conflict Of Interest

The authors declare no conflict of interest.

References

1. R.K. Bindal, I. Kaur, Torque ripple reduction of induction motor using dynamic fuzzy prediction direct torque control, ISA Trans. 99 (2020) 322–338 Available from https://www.sciencedirect.com/science/article/pii/S0019057819304379 .

CC BY SA

2. A. Attar, J. Bouchnaif, K. Grari, Control of brushless DC motors using sensorless Back-EMF integration method, Mater. Today Proc. 45 (2021) 7438–7443 Available from https://www.sciencedirect.com/science/article/pii/S2214785321009585 .
3. S. Jnayah, A. Khedher, Sensorless direct torque control of induction motor using sliding mode flux observer, in: Proceedings of the 2019 19th International Conference on Sciences and Techniques of Automatic Control and Computer Engineering (STA), 2019, pp. 536–541. https://api.semanticscholar.org/CorpusID:159042627.
4. Q. Chen, Y. Xia, J. Wang, W. Zhao, G Liu, Short-circuit fault-tolerant control for five-phase fault-tolerant permanent magnet motors with trapezoidal back-EMF, Fundam.Res.2 (6) (2022) 964–973 Available from https://www.sciencedirect.com/science/article/pii/S266732582100176X .
5. Solly Aryza., Zulkarnain. (2020). Enhance Parameter Speed Estimation of Induction Motor Using Modified Voltage Model Flux Estimation.Jurnal Teknik Elektro dan Telekomunikasi, 7(1),31-35. https://jurnal.pancabudi.ac.id/index.phpeletrotelekomunikasi/article/view/3884
6. Dino Erivianto., Ahmad Dani. (2023). Pelatihan Pemasangan Insulated Gate Bipolar Transistor (Igbt) Inverter Sebagai Pengatur Kecepatan Motor Pada Pt. Prima Multi Peralatan. Pedamas (PengabDian Pada Masyarakat),1(2),421-423. https//pekatpkm.my.id/index.php/JP/article/view/77/54
7. Ahmad Dani., Dino Erivianto.,(2024). Evaluasi Kinerja Motor Induksi Tiga Fasa dengan Modifikasi Resistansi Motor: Pendekatan Simulasi dengan Automation Studio. Journal of Social Science Research.4(3),513. https://jinnovative.org/index.php/Innovative/article/view/12650/855
8. Ahmad Rizal Nurika., Beni Satria., Zulkarnain Lubis. (2024). An Increase Performance Of Unbalanced Induction Motor At High Temperature. Jurnal Scientia.13(2),1318-1322. http://seaninstitute.org/infor/index.php/pendidikan/article/view/2324
9. P. Misra, B. Kumar, Rotor resistance estimation for improved performance of MRAS-based sensorless speed estimation of induction motor drives, in: Intelligent Algorithms for Analysis and Control of Dynamical Systems, Springer Singapore, Singapore, 2021, pp. 177–187, doi:10.1007/978-981-15-8045-1_18. Available from.
10. D.S. Nair, G. Jagadanand, S. George, Torque estimation using Kalman Filter and Extended Kalman Filter algorithms for a sensorless direct torque controlled BLDC motor drive: a comparative study, J. Electr. Eng. Technol. 16 (5) (2021) 2621–2634 Available from, doi:10.1007/s42835-021-00793-7.
11. E. Kuncham, S. Sen, P. Kumar, H. Pathak, An online model-based fatigue life prediction approach using Extended Kalman Filter, Theor. Appl. Fract. Mech. 117 (2022)103143 https://www.sciencedirect.com/science/article/pii/S0167844221002421 .
12. G. Boztas, O. Aydogmus, Implementation of sensorless speed control of synchronous reluctance motor using Extended Kalman Filter, Eng. Sci. Technol. Int. J. 31 (2022) 101066 https://www.sciencedirect.com/science/article/pii/S2215098621001956 .
13. M.G. Hussien, Y. Liu, W. Xu, M.M. Ismail, Voltage regulation-based sensorless position observer with high-frequency signal injection topology for BDFIGs in ship power microgrid systems, Int. J. Electr. Power Energy Syst. 140 (2022) 108091 Available from https://www.sciencedirect.com/science/article/pii/S0142061522001338 .

14. S. Mahfoud, A. Derouich, N. El Ouanjli, M.A. Mossa, S. Motahhir, M. El Mahfoud, et al., Comparative study between cost functions of genetic algorithm used in direct torque control of a doubly fed induction motor, Appl. Sci. 12 (17) (2022) Available from https://www.mdpi.com/2076-3417/12/17/8717 .
15. P.V. de Campos Souza, Fuzzy neural networks and neuro-fuzzy networks: a review the main techniques and applications used in the literature, Appl. Soft Comput. 92 (2020) 106275 Available from https://www.sciencedirect.com/science/article/pii/S1568494620302155 .
16. D. Wachowiak, Genetic algorithm approach for gains selection of induction machine extended speed observer, Energies 13 (18) (2020) (Basel)Available from https://www.mdpi.com/1996-1073/13/18/4632 .
17. I. Benlaloui, L. Chrifi-Alaoui, M. Ouriagli, A. Khemis, D. Khamari, S. Drid, Improvement of the induction motor sensorless control based on the type-2 fuzzy logic, Electr. Eng. 103 (3) (2021) 1473–1482 Available from, doi:10.1007/s00202-020-01178-1.
18. M.J. Karimi, A. Sadighi, M.R.H. Yazdi, Non-intrusive induction motor parameter estimation using MRAS algorithm and neural network rotor flux observer, in: Proceedings of the 2022 10th RSI International Conference on Robotics and Mechatronics (ICRoM), 2022, pp. 267–272. https://api.semanticscholar.org/CorpusID:256463042. Available from
19. S. Rubino, R.I. Bojoi, F. Mandrile, E Armando, Modular stator flux and torque control of multiphase induction motor drives, in: Proceedings of the 2019 IEEE International Electric Machines & Drives Conference (IEMDC), 2019, pp. 531–538. https://api.semanticscholar.org/CorpusID:199489721. Available from
20. J. Bonet-Jara, A. Quijano-Lopez, D. Morinigo-Sotelo, J. Pons-Llinares, Sensorless speed estimation for the diagnosis of induction motors via MCSA. Review and commercial devices analysis, Sensors 21 (15) (2021) Available from https://www.mdpi.com/1424-8220/21/15/5037.
21. U. Sengamalai, G. Anbazhagan, T.M. Thamizh Thentral, P. Vishnuram, T. Khurshaid, S Kamel, Three phase induction motor drive: a systematic review on dynamic modeling, parameter estimation, and control schemes, Energies 15 (21) (2022) (Basel)Available from https://www.mdpi.com/1996-1073/15/21/8260.
22. S. Rajendran, M. Diaz, R. Cárdenas, E. Espina, E. Contreras, J. Rodriguez, A review of generators and power converters for multi-mw wind energy conversion systems, Processes 10 (11) (2022) 2302, https://doi.org/10.3390/pr10112302.
23. J.D. Camelo-Daza, D.N. Betancourt-Alonso, O.D. Montoya, E. Gómez-Vargas, Parameter estimation in single-phase transformers via the generalized normal distribution optimizer while considering voltage and current measurements, Results Eng. 21 (2024) 101760, https://doi.org/10.1016/j.rineng.2024.101760.
24. L. Abualigah, M. Altalhi, A novel generalized normal distribution arithmetic optimization algorithm for global optimization and data clustering problems, J. Ambient Intell. Humaniz. Comput. (2022), https://doi.org/10.1007/s12652-022-03898-7.
25. J.A. Vega-Forero, J.S. Ramos-Castellanos, O.D. Montoya, Application of the generalized normal distribution optimization algorithm to the optimal selection of conductors in three-phase asymmetric distribution networks, Energies 16 (3) (2023) 1311, https://doi.org/10.3390/en16031311.

CC BY SA

26. O.D. Montoya, L.F. Grisales-Noreña, C.A. Ramos-Paja, Optimal allocation and sizing of pv generation units in distribution networks via the generalized normal distribution optimization approach, Computers 11 (4) (2022) 53, https://doi.org/10.3390/computers11040053.
27. M.O. Gülbahçe, M.E. Karaaslan, Estimation of induction motor equivalent circuit parameters from manufacturer's datasheet by particle swarm optimization algorithm for variable frequency drives, Electrica 22 (1) (2021) 16–26, https://doi.org/10.5152/electrica.2021.21122.
28. G. Rigatos, M. Abbaszadeh, P Siano, A nonlinear optimal control approach for permanent magnet AC motors with non-sinusoidal back EMF, Electr. Eng. 104 (4) (2022) 2293–2318 Available from, doi:10.1007/s00202-021-01475-3.
29. G. Wang, H Zhang, A new speed adaptive estimation method based on an improved flux sliding-mode observer for the sensorless control of PMSM drives, ISA Trans. 128 (2022) 675–685 Available from https://www.sciencedirect.com/science/article/pii/S0019057821004870 .
30. K. Laadjal, F. Bento, H.R.P. Antunes, M. Sahraoui, A.J.M. Cardoso, Speed estimation of six-phase induction motors, using the rotor slot harmonics, Sensors 22 (21) (2022 Oct) 8157 (Basel)Available from https://europepmc.org/articles/PMC9656993 .
31. S.D. Niño-Callejas, J.C. Palombi-Gómez, O.D. Montoya, Applying the sine-cosine optimization algorithm to the parametric estimation problem in three-phase induction motors, Ing. Investig. 44 (2) (2024) 1–11, https://doi.org/10.15446/ing.investig. 110310.
32. C. Terron-Santiago, J. Martinez-Roman, R. Puche-Panadero, A. Sapena-Bano, A review of techniques used for induction machine fault modelling, Sensors 21 (14) (2021) 4855, https://doi.org/10.3390/s21144855.
33. J. Montano, O.D. Garzón, D.A. Herrera-Jaramillo, O.D. Montoya, F. Andrade, A. Tobon, Estimating the parameters of a three-phase induction motor using the vortex search algorithm, Iran. J. Sci. Technol. Trans. Electr. Eng. (2023), https://doi.org/10.1007/s40998-023-00673-y.
34. S.Y. Bocanegra, O.D. Montoya, A. Molina-Cabrera, Parameter estimation in singlephase transformers employing voltage and current measures, Rev. UIS Ing. 19 (4) (2020) 63–75, https://doi.org/10.18273/revuin.v19n4-2020006.
35. K.M. Charu, P. Thakur, N. Rawat, F. Ansari, S. Gupta, M. Kumar, An efficient data sheet based parameter estimation technique of solar pv, Sci. Rep. 14 (1) (Mar. 2024), https://doi.org/10.1038/s41598-024-57241-5.

CC BY-SA 4.0 (Attribution-ShareAlike 4.0 International).
This license allows users to share and adapt an article, even commercially, as long as appropriate credit is given and the distribution of derivative works is under the same license as the original. That is, this license lets others copy, distribute, modify and reproduce the Article, provided the original source and Authors are credited under the same license as the original.